Carbon Nanotube Translocation to Distant Organs after Pulmonary Exposure: Insights from *in Situ* ^{14}C-Radiolabeling and Tissue Radioimaging

Bertrand Czarny,[†] Dominique Georgin,[‡] Fannely Berthon,[†] Gael Plastow,[†] Mathieu Pinault,[§] Gilles Patriarche,[∥] Aurélie Thuleau,[†] Martine Mayne L'Hermite,[§] Frédéric Taran,[‡] and Vincent Dive[†,*]

[†]CEA-Saclay, Service d'Ingénierie Moléculaire des Protéines, Labex LERMIT, CEA-DSV-iBiTecS, 91191 Gif/Yvette, France, [‡]Service de Chimie Bioorganique et de Marquage, CEA-Saclay, CEA-DSV-iBiTecS, 91191 Gif/Yvette, France, [§]Laboratoire Francis Perrin (CNRS URA 2453), CEA-Saclay, CEA, IRAMIS, NIMBE, 91191 Gif/Yvette, France, and [∥]Laboratoire de Photonique et de Nanostructures, CNRS-LPN, Route de Nozay, 91460 Marcoussis, France

ABSTRACT

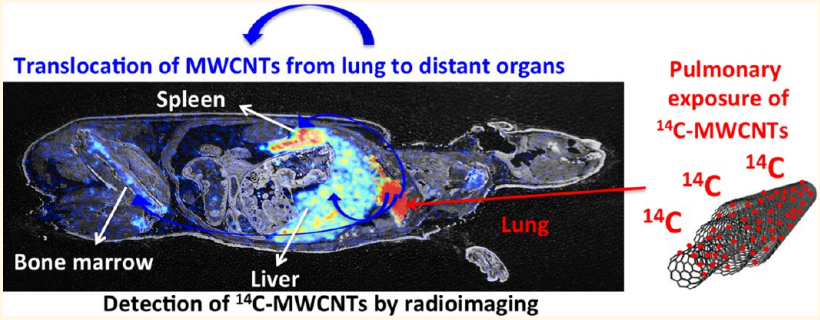

Few approaches are available to investigate the potential of carbon nanotubes (CNTs) to translocate to distant organs following lung exposure, although this needs to be taken into account to evaluate potential CNT toxicity. Here, we report a method for quantitative analysis of the tissue biodistribution of multiwalled CNTs (MWCNTs) as a function of time. The method relies on the use of *in situ* ^{14}C-radiolabeled MWCNTs and combines radioimaging of organ tissue sections to *ex vivo* analysis of MWCNTs by electron microscopy. To illustrate the usefulness of this approach, mice were exposed to a single dose of 20 μg of ^{14}C-labeled MWCNTs by pharyngeal aspiration and were subjected to a follow-up study over one year. After administration, MWCNT were cleared from the lungs, but there was a concomitant relocation of these nanoparticles to distant organs starting throughout the follow-up period, with nanoparticle accumulation increasing with time. After one year, accumulation of MWCNTs was documented in several organs, including notably the white pulp of the spleen and the bone marrow. This study shows that the proposed method may be useful to complement other approaches to address unresolved toxicological issues associated with CNTs. These issues include their persistence over long periods in extrapulmonary organs, the relationship between the dose and the extent of translocation, and the effects of "safety by design" on those processes. The same approach could be used to study the translocation propensity of other nanoparticles containing carbon atoms.

KEYWORDS: carbon nanotube · air–blood barrier · translocation · *in vivo* biodistribution · ^{14}C-radiolabbeling, radioimaging

Carbon nanotubes (CNTs) are very promising for a variety of industrial and biomedical applications due to their physicochemical properties.[1,2] As a result, many different types of CNTs have been produced on an industrial scale over the last 20 years, raising the issue of their safety.[3,4] Most studies addressing their effects on health have focused on the potential respiratory toxicity of CNTs in an occupational context, during their production and processing.[5,6] Early studies in animal models demonstrated that CNTs can cause pulmonary inflammation, lung and subpleural fibrosis, alterations of the oxidant/antioxidant balance, and cardiovascular and immunosuppressive effects.[7−10] Toxicological responses to CNTs can differ according to the dose, route of

* Address correspondence to vincent.dive@cea.fr.

Received for review January 24, 2014 and accepted May 22, 2014.

Published online May 22, 2014
10.1021/nn500475u

exposure, and type of CNT (morphology, structure, diameter, length, and surface chemistry).[11] The possible formation of CNT agglomerates in tissue is also thought to contribute to the toxicity outcomes, their clearance by macrophages, and their interaction with the biological environment (mucus, plasma, protein corona).[12,13] After deposition in the lungs, nanoparticles can be cleared through several processes or may be redistributed to other tissues if they cross the air−blood barrier.[14] Translocation of multiwalled CNTs (MWCNTs) to lymph nodes[15,16] and pleural sites has been documented,[17,18] and more recently translocation to organs distant from lungs has been reported.[19,20] The latter study was based on the direct observation of CNTs in tissue sections by enhanced dark-field microscopy involving counting CNTs per unit area and the extrapolation of CNT quantity per organ using a morphometric method. Although this approach allowed very high sensitivity (a single CNT is detected), it was extremely time-consuming, as it required the processing and analysis of a huge number of tissue sections. As an alternative, we have developed a method involving ^{14}C-labeled MWCNT and radioimaging of tissue sections to detect translocation of these nanoparticles in organs distant from lungs. The main objective of this project was to evaluate whether this approach is feasible and sufficiently sensitive to detect translocation events. Toxicity was not an issue of this study.

RESULTS AND DISCUSSION

CNTs have previously been labeled with ^{14}C by attaching a radioactive tag onto their surface.[21] This approach suffers from the potential instability of the tagging and also the possible alteration of the physicochemical properties of CNTs. These drawbacks may change both CNT bioactivity and *in vivo* biodistribution. To avoid these problems, *in situ* radiolabeling of MWCNT with ^{14}C by a catalytic chemical vapor deposition (CCVD) method, using methane as carbon source, has been described. However, this first attempt resulted in ^{14}C-labeling of MWCNTs at a low specific activity (4.5×10^3 Bq/mg).[22] To increase the specific radioactivity substantially, we used ^{14}C-labeled benzene as the carbon source rather than the ^{14}C-labeled methane used previously, together with the aerosol-assisted CCVD process.[23,24] Using these conditions, the specific activity of the resulting ^{14}C-MWCNTs (10×10^6 Bq/mg) was more than a thousand times higher and corresponded to a ^{14}C/^{12}C ratio of approximately 1/17. Consequently, with this unprecedentedly high specific activity, as little as 0.2 pg of MWCNTs can be detected with a sensitive radioimager, corresponding to a detection threshold of approximately 22 CNTs (Figure 1a,b) (The weight of an MWCNT of 3.9 μm length and 41 nm diameter (density measured = 1.8) is around 9×10^{-15} g.) Similar detection thresholds were obtained when CNTs were spotted either directly on a glass support (Figure 1a) or onto tissue sections (Figure 1b). Transmission electron microscopy (TEM) of bulk ^{14}C-labeled MWCNTs showed an average external diameter of 40 nm (Figure 1c; see Materials and Methods section for additional characterization of MWCNTs). These bulk MWCNTs were used for animal studies without postsynthesis treatment such as purification in acidic media, which strongly affects the surface chemistry of CNTs. The administration procedure of CNTs in animals necessitates the preparation of suspensions, which was performed in a biocompatible medium as previously reported.[25] Optical microscopy and TEM revealed that the MWCNTs were well dispersed in this medium, with only a few agglomerates (Figure 1d). After dispersion, CNT lengths vary from 500 nm to 12 μm (mean length 3.9 μm) and diameters from 10 to 150 nm, centered on 40 nm (Figure 1e).

Female Balb/c mice were exposed to a single dose of pristine ^{14}C-labeled MWCNTs by pharyngeal aspiration; the dose administered was the same as one of the lower doses previously used by Porter *et al.* in mice (20 μg, 196×10^3 Bq).[8] Compared to inhalation, this protocol involves a rapid bolus deposition of MWCNTs in the lung,[26] but it was chosen because the applied dose is more easily controlled. Also, the amount of radioactive MWCNT available for this first study was too limited to use inhalation for animal exposure. Mice were sacrificed at 1 and 7 days and 1, 3, 6, 9, and 12 months (4 animals/time point) after exposure, and tissue sections of lung, liver, spleen, kidney, brain, heart, thymus, and bone marrow were processed for analysis. The tissue sections were analyzed by quantitative radioimaging to observe changes in radioactivity as a function of time (lymph nodes were not included in this study, as the translocation of MWCNT from lung to these organs has already been documented). Blood and urine samples were collected at the same time points and analyzed for radioactivity content. No radioactive signal was detected in urine and in blood at day 1 after exposure (Figure 2a and b). Thus, radioactive signals in tissue sections after day 1 cannot be accounted for by blood contamination. Radioimaging data indicated a decrease of the radioactive signal in lung tissue sections from day 1 to day 90 (Figure 2c) and an increase in spleen and liver from day 7 to day 360 (Figure 2d). In kidney and bone marrow, a radioactivity increase was also observed but to a lesser extent as compared to liver and spleen (Figure 2d and Figure S1, Supporting Information). In spleen and liver, at a higher sensitivity scale, a radioactive signal was detected at day 1 (Figure 2e). Radioimaging of spleen and bone tissue sections at higher resolution revealed that MWCNTs were concentrated in the white pulp of spleen (Figure 2f, left) and in bone marrow (Figure 2f, right).

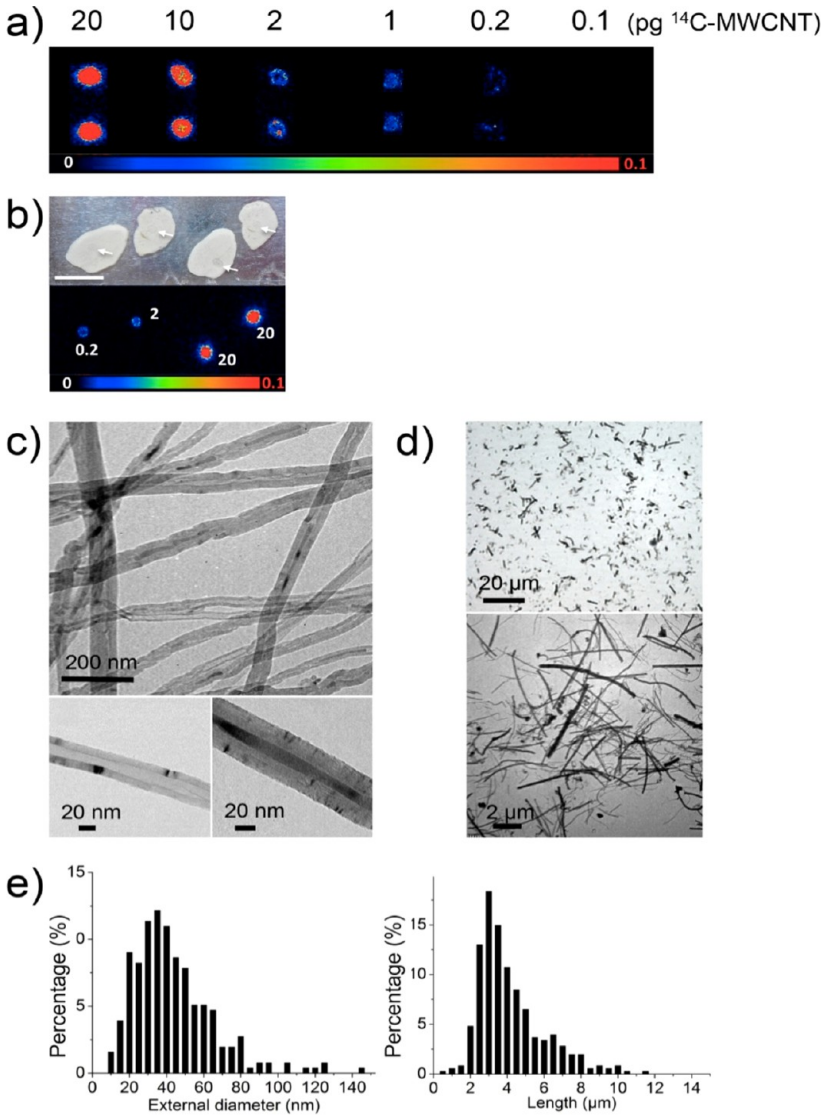

Figure 1. (a) Detection threshold of ^{14}C MWCNTs by radioimaging; 20, 10, 2, 1, and 0.2 pg of ^{14}C-MWCNTs were spotted on a glass support. (b) Upper panel: optical images of liver tissue sections on which were spotted ^{14}C-MWCNTs (white arrow), lower panel: corresponding radioimaging analysis (numbers corresponds to pg of ^{14}C-MWCNTs). (c) TEM images of ^{14}C-MWCNTs as produced and (d) as suspended in dispersion medium (upper panel optical image, lower panel TEM image. (e) Diameter and length distribution of ^{14}C-MWCNTs in dispersion medium.

Radioactivity counting cannot distinguish between radioactive signals corresponding to MWCNTs and those from potential metabolites. The slow redistribution of radioactivity from lung to spleen and liver over a one-year period does not argue for small metabolite occurrence, as such potential metabolites would be expected to relocate rapidly and be rapidly and completely cleared after exposure.[27] Furthermore, the absence of radioactive signals in urine does not support the *in vivo* metabolite formation from MWCNTs, as most polar compounds resulting from MWCNT oxidation would be cleared and observed in urine. It is worth noting that degradation products were reported under *in vitro* conditions and only for single-walled nanotubes.[28,29] To further check for the absence of metabolites, tissue extracts were analyzed by thin-layer chromatography (TLC) and radioimaging. MWCNTs did not migrate on the TLC plate; they were thus detected at the deposit point. In contrast, metabolites if present should migrate on the TLC plate, as shown for the ^{14}C 2,4-dimethoxybenzoic acid compound (Figure S2, Supporting Information), which was selected as one potential MWCNT degradation product. No signal of radioactivity was detected above the tissue extract signals of spleen and liver (12 months postinjection). Given the detection threshold of radioimaging, 1% degradation of MWCNTs would have generated detectable metabolites. However, keeping in mind the ratio in ^{14}C-MWCNTs of one ^{14}C-carbon for 17 ^{12}C-carbons, we cannot totally exclude the formation of ^{12}C metabolites, not observable under our analytical experiments. Nonetheless, an estimation of

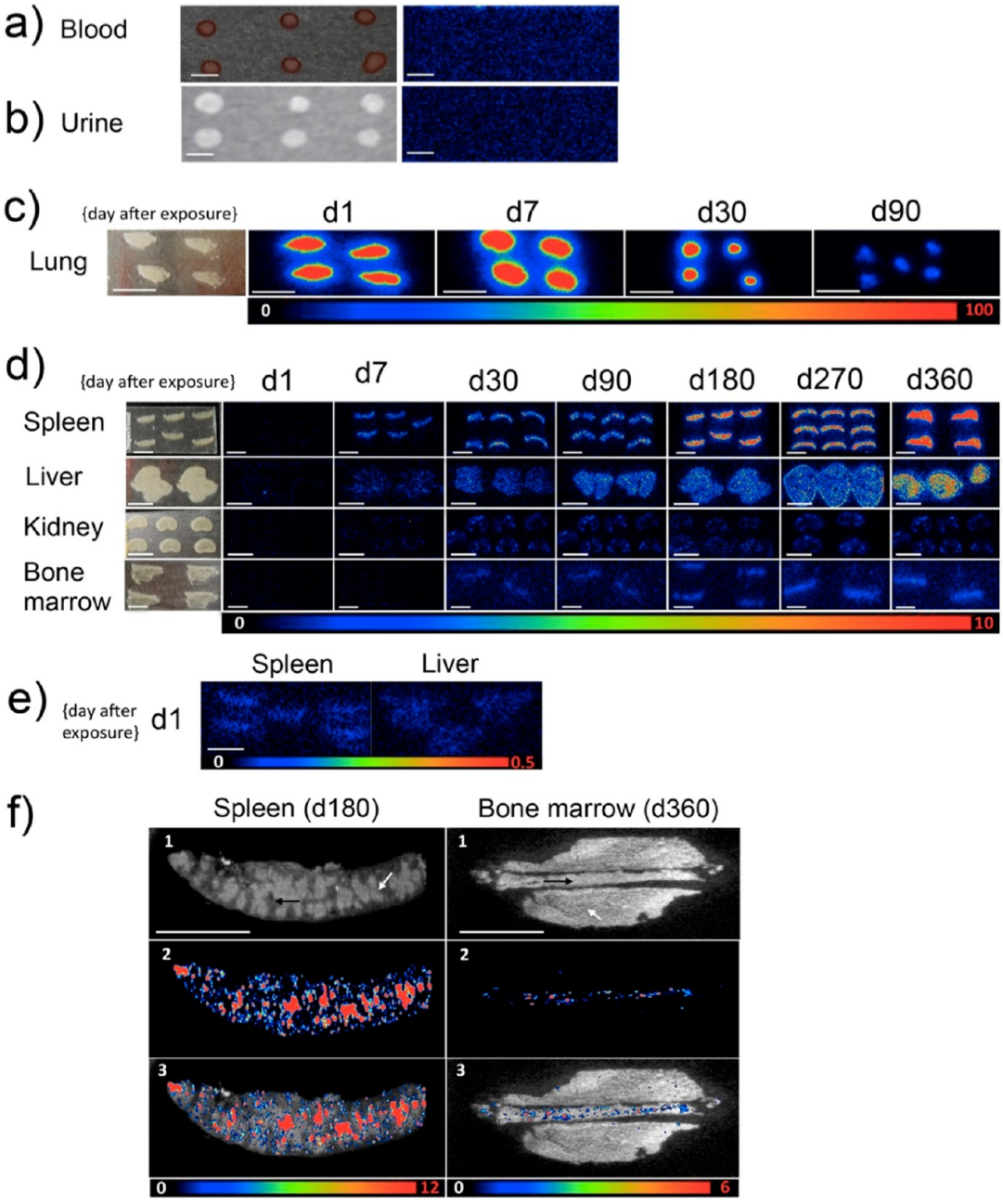

Figure 2. (a and b) Blood and urine samples taken from mice at day 1 after ^{14}C-MWCNT lung exposure, optical images of spotted samples are shown on the left and the corresponding radioimaging is reported on the right: no radioactivity was detected in these samples. (c and d) After ^{14}C-MWCNT lung exposure, four to six pieces of tissue sections from mice were placed on a glass support (optical images on the left) and were analyzed by radioimaging from day 1 to day 360 postexposure. While the radioactive signal decreased in lung, it increased in spleen, liver, kidney, and bone marrow. (e) radioimaging of spleen and liver tissue sections at day 1 postexposure, at the highest detection sensitivty. (f) High-resolution radioimaging of spleen and bone tissue sections at day 360 postexposure revealed the presence of radioactivity in the white pulp of spleen (white arrow) and in bone marrow; upper panel optic image, middle panel radioimaging, and lower superimposition of both images. White bars 1 cm, except for (f) 0.5 cm; color bar under radioimaging codes for the radioactive intensity scale.

the MWCNT quantities that have translocated to spleen and liver was performed considering that metabolite formation was unlikely (see paragraph on the *ex vivo* characterization of MWCNTs).

The total quantity of MWCNT present in organs was estimated by summing the signal obtained for 50 tissue sections chosen to sample the organ and extrapolating this signal to the whole organ. The resulting value for the total radioactivity per organ was then converted to a quantity of MWCNT using the specific radioactivity. This approach assumes a homogeneous distribution of MWCNTs throughout the whole organ. However, the aspiration protocol used to administer the MWCNTs does not result in a

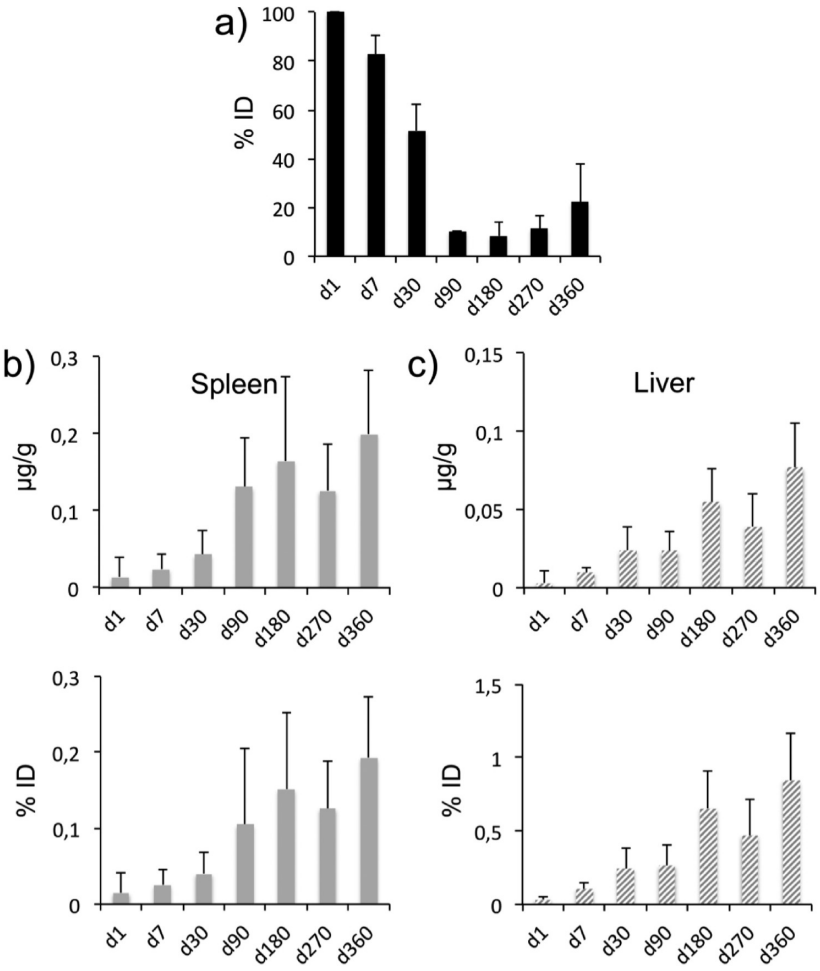

Figure 3. Percentage of the administered dose (100%, 10 μg) at various times after lung exposure of mice to ^{14}C MWCNTs in (a) lung, (b) spleen, and (c) liver; in (b) and (c), the upper panel reports the quantity of MWCNTs in μg/g of tissue; the lower panel reports % of the injected dose. Data are mean $\pm$ SEM, n = 4 mice.

homogeneous distribution in the lung. Thus, for this organ, MWCNTs were extracted and the radioactivity in the extracts was counted by the liquid scintillation method (see Materials and Methods). For spleen and liver, half of the organ was analyzed by radioimaging and the other half by liquid scintillation counting, allowing for comparison of the two procedures. For an MWCNT quantity up to 5 ng/g of tissue, the two methods gave similar results with an uncertainty of $\pm$10%. These quantification procedures indicated that the lung burden on day 1 was about 10 μg of MWCNTs. As only half of the administered MWCNTs were found in the lung on day 1, it is likely that, in addition to MWCNT clearance from the lung by mucociliary transport, most probably a significant proportion of the applied dose has been swallowed, ending up in the stomach/gastrointestinal tract. The applied dose in the lung was thus set to 10 μg (100%), and this value was used to normalize all data. In month 3 and latter up to month 12, about 10% of the dose applied remained in the lung (1 μg) (Figure 3a). On a gram basis, the spleen accumulated more MWCNTs than the liver, with 200 ng and 75 ng of MWCNTs detected at month 12 in these tissues (Figure 3b and c upper), corresponding respectively to 0.2% and 0.75% of the administered dose (Figure 3b and c, bottom). Twelve months postexposure, substantially less radioactivity was detected in heart and none was detected in brain and thymus (Figure S3, Supporting Information).

TEM can be used to visualize CNTs in tissue sections, but this approach would suffer from the extremely low concentration of CNTs in the sectioned organs, as indicated by radioactivity counting. Therefore, MWCNTs were extracted from tissue samples and concentrated before TEM imaging. MWCNTs were successfully isolated from lung 12 months postexposure and analyzed by TEM, revealing MWCNTs of various diameters and lengths (0.2$-$10 μm; Figure 4a$_1$). High-resolution TEM allowed visualizing the different layers of CNTs and the determination of their diameters (Figure 4a$_2$ and a$_3$). In spleen extracts from animals 12 months after MWCNT exposure, measurements indicated the presence of particles with a diameter of 40 nm (Figure 4b), similar to the administered bulk MWCNTs. Black contrast observed inside the hollow core of nanotubes was attributed to iron-based

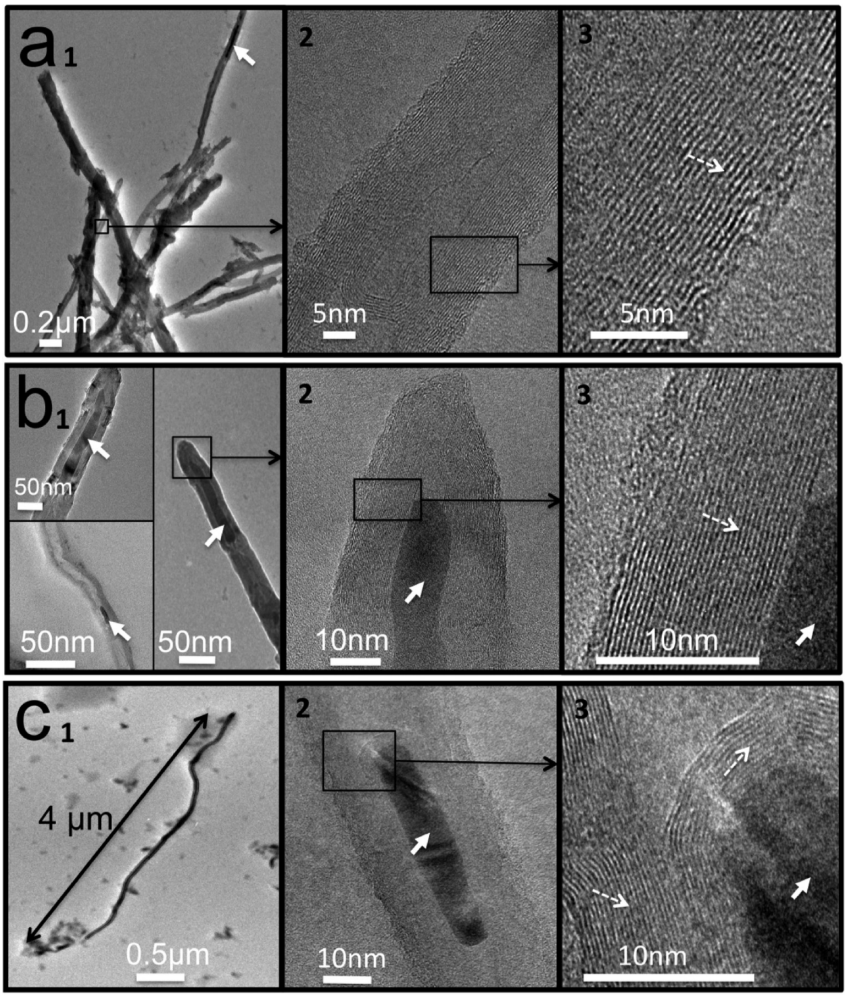

Figure 4. TEM images of ^{14}C-MWCNTs 12 months postexposure in (a) lung, (b) spleen, and (c) liver at different resolution from low (subscript 1) to high resolution (subscript 3). In the lung, MWCNTs with different diameters (from 25 to 60 nm) and lengths (from 300 nm to 1 μm) were observed. In spleen (b), several MWCNTs with 40 nm diameter were observed, and in the liver (c), a 4 μm length MWCNT was observed. Dashed arrows indicate carbon walls; bold arrows indicate iron clusters.

particles by EDX elemental mapping (Figure 4b,c). Given the ^{14}C/^{12}C ratio of approximately 1/17 in these MWCNTs, the isolated MWCNTs are necessarily radioactive nanotubes and accounted thus for the presence of a radioactive signal in the tissue sections. Long MWCNTs were found to have translocated, as revealed by the observation of a nanotube of 4 μm length in liver extracts (Figure 4c). As calculated from the mean mass of individual MWCNTs (9×10^{-15}g) and the percentage of the injected dose found in organs after 12 months, each mouse spleen retained about 20 ng and liver 75 ng of CNTs, corresponding to $\sim 2 \times 10^6$ and $\sim 8 \times 10^6$ of individual nanotubes, respectively.

As mentioned before, part of the MWCNTs have been cleared by the gastrointestinal tract, so translocation processes may have taken place across intestinal barriers. To rule out this possibility, oral ingestion of MWCNTs through intraesophageal instillation has been performed, using a higher dose of MWCNTs (50 μg) to detect low levels of translocation across the intestinal barriers. After 24 h, 95 $\pm$ 15% of ingested MWCNT dose was found in the gastrointestinal tract and feces (Figure S4, Supporting Information). After 4 days, no more radioactivity was evidenced in the gastrointestinal tract and feces (data not shown). At the highest scale of sensitivity, no radioactive signal was observed by radioimaging in spleen and liver tissue sections 1, 7, and 30 days after MWCNT gavage (Figure S4, Supporting Information). These observations are in contrast with the presence of radioactive signals in spleen and liver tissue sections after lung exposure to MWCNTs at a lower dose (10 versus 50 μg). These results thus validated the proposal that the translocation observed after lung exposure is due only to a translocation of MWCNTs through the air–blood barrier and not across intestinal barriers. Over the whole experimental period, the 10% of MWCNTs remaining in the lung should act as a reservoir for the translocation process to distant organs.

To reach blood and lymph circulation, MWCNTs must cross the epithelial layer of the airways or the alveoli, an event that can be regulated by the relative

size of the pores at this barrier. The maximum pore radius estimated for the alveolar epithelium is on the order of 1 to 5 nm and radii from 7 to 12 nm for airways.[30] However, the occurrence of large-sized pores (400 nm pores radius) and medium-sized pores (40 nm) has been suggested, explaining the fast passage through the alveolar-airway barrier of proteins with a mean radius greater than 50 nm.[31] These pores may explain the fast translocation to the bloodstream of spherical gold nanoparticles of 80 nm diameter to lung-distant organs 1 h after intratracheal instillation.[32] Translocation of MWCNTs at day 1 postexposure may take place through these functional pores. After these initial events, at later times postexposure, alteration of the air−blood barrier may facilitate further passage of MWCNTs in the blood.

While this paper was in preparation, Mercer *et al.* reported translocation of MWCNTs in mice after exposure by inhalation.[20] The mice were exposed in a whole-body inhalation system to a 5 mg/m^3 MWCNT aerosol for 5 h/day during 12 days (lung burden 28.1 μg/lung) and were analyzed at only two time points, 1 and 336 days after the 12-day exposure period. Although the exposure protocols and the source of MWCNTs were very different, both our study and that by Mercer *et al.* led to similar qualitative conclusions: MWCNTs are translocated from the lung to several distant organs. Nonetheless, differences between the two studies should be highlighted. In the study by Mercer *et al.*, the extent of MWCNT translocation was much lower: they found 0.03% of the lung burden in the liver on day 336, whereas in our study after one year almost 0.75% of the dose applied was observed in the liver. For the spleen, a major site of accumulation in our study, their results were very different, as no MWCNTs were detected in this organ. As mentioned above, these divergences can be explained on the basis of the differences between the MWCNTs used in the two studies. In addition the larger extent of MWCNT translocation to distant organs in our study could be due to our exposure protocol involving a bolus injection of MWCNT, resulting in a different distribution of nanoparticles within the lung, as compared to inhalation. Different routes by which MWCNTs are transported to distant organs have been discussed in the paper of Mercer *et al*, but the exact scenario cannot be determined with current data. Future experiments will have to determine if CNTs are traveling into blood circulation as single particles or by macrophage-mediated transport. Analysis of tissue sections by different imaging methods will be necessary to give a precise description of the location of MWCNTS in lung and distant organs. If easily feasible for lung tissues, these experiments will be much more difficult to perform in the spleen and liver given the extremely low number of MWCNTs in these organs. It is worth noting that when MWCNTs were iv injected, at day 1 after administration, MWCNTs were observed to target preferentially the liver, then the spleen and to a lesser extent the lung (Figure S5, Supporting Information). This biodistribution is different from that reported after lung exposure (Figure 3c and d). Similar results were previously reported for other nanoparticles, and to explain these differences it has been proposed that the administration mode may determine the content of proteins at the MWCNT surface and that this "protein corona" may govern biodistribution.[33]

The main focus of our study was not to draw toxicological conclusions, but to demonstrate that combining radiolabeling and radioimaging is a feasible alternative or complementary approach to that used by Mercer *et al.*[20] Due to the straightforward tissue handling and biodistribution analysis by quantitative radioimaging, our approach can be used for follow-up studies, sampling animals at numerous time points over a long period, rather than at only two time points (d 1 and d 336 after 12 days of exposure in the study by Mercer *et al.*), and to obtain quantitative data without laborious work. With some adaptations, to reduce the amount of MWCNTs required, study of inhaled radiolabeled MWCNTs seems possible. Our data confirm that translocation can be observed even 1 day after the exposure and, in addition, that accumulation of MWCNTs in distant tissues increased for up to one year after exposure, with no decrease in spleen or liver. It will be important in future studies to investigate whether a clearance of these particles after this period can take place in these distant organs and on what time scale, or if they persist. The sensitivity of our approach, 22 MWCNTs rather than 1 in Mercer's study, is sufficient to detect a few nanograms of MWCNT in a whole organ or a few picograms in a tissue section. Radioimaging at high resolution of spleen tissue sections revealed preferential localization of the MWCNTs in the white pulp (Figure 2f), a key tissue structure for immune surveillance. It has been reported that exposure of mouse lungs to MWCNTs can alter the immune system 30 days postexposure, through molecular signals from the lung that turn on signals directly in the spleen.[33] We reported on the presence of MWCNTs in spleen on day 1 postexposure (Figure 2e) and their steady bioaccumulation in this organ up to month 12; it is therefore possible that the presence of MWCNTs in the white pulp of spleen may have a direct role in long-term immunosuppressive effects.

A similar approach could be used to determine how the size (length and diameter) of MWCNTs influences the efficiency and kinetics of their translocation. Such experiments could be used to screen many different MWCNTs, as translocation is rapid and our approach is sufficiently sensitive to detect early translocation events. Similarly, for nanomedicine applications, the effect of the surface chemistry, and particularly its consequences for translocation properties, could be assessed.[2] The same

approach could be applied to graphene, to assess its suitability for biomedical applications,[34] and to other nanoparticles containing carbon atoms.

CONCLUSION

The present study describes how radioimaging of tissue sections can be used to rapidly determine the biodistribution of ^{14}C-MWCNTs. After pharyngeal aspiration of ^{14}C-MWCNTs to mice, a small amount of the applied MWCNT dose was observed to translocate to distant organs, showing the capacity of MWCNTs to cross the air−blood barrier. MWCNTs were observed to increasingly accumulate in these peripheral organs such as spleen and bone marrow over the whole period of this study, from day 1 to month 12, with no decrease observed, leading us to conclude that a biopersistence of these nanoparticles in these secondary organs exists.

MATERIALS AND METHODS

^{14}C-Labeled Multiwalled Carbon Nanotube Synthesis. ^{14}Carbon-labeled carbon nanotubes were synthesized by a chemical vapor deposition process specifically developed for the use of ^{14}C benzene as carbon source. The standard experimental setup involves an aerosol generator,[23,24] a quartz reactor placed in a furnace, and traps for the exhaust gases and was appropriately modified to be used with small amounts of radioactive liquid carbon precursor. A mixture of 0.5 mL of ^{14}C-benzene (4.63 GBq/mmol, radiochemical and chemical purity >99.9%, from Quotient Bioresearch Radiochemicals Ltd.) and 1.5 mL of benzene (Sigma) containing 4% (w/w) ferrocene was placed in a reservoir and injected over 18 min as an aerosol carried by argon (argon flow = 1 L/min) into the quartz reactor in a furnace at 850 °C. After cooling, the black powder covering the internal surface of the reactor was collected to obtain 25 mg of carpet pieces in the isothermal zone of the reactor. These carpet pieces were analyzed by scanning electron microscopy (SEM) (JEOL 5400) and transmission electron microscopy (TEM) (Philips CM 30; CEA Saclay, DEN-LM2E, France) and found to be mainly composed of vertically aligned MWCNTs, 50 μm thick, with almost no by-products (such as amorphous carbon). From these observations, iron-based particles were mostly observed at the base and inside the hollow core of the MWCNTs. Thermogravimetric analysis (TGA 92-16, 18 SETARAM apparatus) was used to determine the global iron content in the samples by measuring the remaining iron oxide weight resulting from the oxidation of iron during TGA treatment under air. Thermogravimetric analysis of nonradioactive MWCNT samples (synthesized in similar conditions to those for the ^{14}C-labeled MWNTs) under flowing air at a temperature up to 1000 °C (10 °C min^{-1} heating ramp) was used to determine the initial iron content of the samples by measuring the remaining iron oxide weight. The iron concentration was *ca.* 7.4 wt %. The chemical composition of the nonradiolabeled MWCNT surface was evaluated by XPS (X-ray-induced photoelectron spectroscopy) analysis using a Kratos Analytical Axis Ultra DLD spectrometer with monochromatic Al Kα X-ray radiation ($h\nu$ = 1486.6 eV). Quantitative analysis indicated that the C content was *ca.* 98.36 at. % and the O content was *ca.* 1.64 at. %, with a major contribution of C sp^2 and minor contributions of C sp^3 and C-OOH groups. Their specific surface area was 42 ± 2 m^2/g.

Preparation and Characterization of ^{14}C-MWCNT Suspensions. Two milligrams of ^{14}C-MWCNT was added to 5 mL of dispersion medium (calcium- and magnesium-free phosphate-buffered saline, pH 7.4, supplemented with 5.5 mM D-glucose, 0.6 mg/mL mouse serum albumin, and 0.01 mg/mL 1,2-dipalmitoyl-*sn*-glycero-3-phosphocholine).[25] The suspension was dispersed by high-energy ultrasound (Autotune 750 W, Bioblock Scientific) at 4 °C for 1 h, in pulsed mode (1 s on, 1 s off, 28% of the maximal amplitude). This protocol was chosen to adjust MWCNT length in the final suspension, as high-energy ultrasound treatment induces CNT breaking. Optical microscopy and high-resolution TEM were used to characterize the length and diameter distribution of MWCNTs when suspended in dispersion medium and their dispersion state. A droplet of the MWCNT suspension was deposited on a TEM grid, allowed to evaporate for 1 min, and then washed three times with ultrapure water. For optical microscopy (Olympus BX60 microscope), a droplet of the MWCNT suspension was deposited on a glass slide, allowed to dry for 5 min, and then protected with a coverslip. The length and diameter of 150−200 randomly chosen MWCNTs were measured by both techniques. In addition to individualized MWCNTs, a few agglomerates of longer nanotubes were observed. Endotoxin concentrations in these samples were below the threshold of detection, using the Limulus amebocyte lysate assay (Kinetic-QCL, BioWhittaker).

General Procedure for *in Vivo* Experiments. *Animals.* Pathogen-free, 6-week-old, female Balb/c mice weighing 20 g (Charles River Laboratories, L'Arbresle, France) were individually housed in polycarbonate cages in a conventional animal facility and had access *ad libitum* to food and drink. The local ethics committee for animal experimentation approved the experimental protocol.

Dosing and Biodistribution Analyses. Lung Exposure. Seven groups of mice (n = 4) were exposed by pharyngeal aspiration to 20 μg of ^{14}C- MWCNTs (285 × 10^3 Bq), suspended in dispersion medium (50 μL). The suspension was prepared immediately before administration. Mice were anesthetized with 2% isoflurane and suspended by their upper incisors from a rubber band on a board inclined at 60°. The tongue was gently extended and the MWCNT solution (50 μL) was delivered into the distal part of the oropharynx, such that the liquid was drawn into the lower respiratory tract by aspiration. Mice were sacrificed 1 and 7 days and 1, 3, 6, 9, and 12 months after lung exposure to MWCNTs. Blood was collected by exsanguination; then all organs were collected and immediately frozen at −80 °C by immersion in a mixture of dry ice and isopentane to prevent redistribution of the MWCNTs. Half of the analyzed organs were maintained in mounting medium, and tissue sections (20 μm thick) were cut at −20 °C with a slicing microtome (LEICA Microsystems, France). The microtome was carefully cleaned by water−ethanol solution between treatment of each sample to remove any trace of radioactivity and avoid contamination between different organs. The absence of radioactive contaminants in the rinsing solution was controlled by radioimaging of drop samples. The tissue sections were placed on glass slides and were either stored in a freezer for optical study or kept at room temperature for 1 day in the presence of silica gel to ensure complete drying for proper radioimaging analysis. A high-performance autoradiography imager (β-imager 2000, Biospace Lab, Paris, France) allowing real-time radioactive imaging through direct β-particle counting and absolute radioactivity quantification[35] (detection threshold of 0.01 cpm/mm^2 for ^{14}C) was used for quantitative determination of the radioactivity in dried tissue sections. Correct calibration of the apparatus was verified between each sample analysis by counting the radioactivity of a reference sample (blood with known quantity of ^{14}C-MWCNT). For superposition of microscope and autoradiographic images, the tissue sections of interest were analyzed with a μ-imager (Biospace Lab, Paris, France) to determine the tissue distribution of the radioactivity with a resolution down to 15 μm.

Gavage. Three groups of mice (n = 6) were exposed by gavage to 50 μg of ^{14}C- MWCNTs (714 × 10^3 Bq), suspended in dispersion medium (100 μL). After administration of the CNT suspensions, mice were kept individually in metabolism cages for separate collection of urine and feces. Feces and urine was collected each day. Six mice were sacrificed at 1, 7, and 30 days

after exposure to MWCNTs. Blood was collected by exsanguination; then all organs were collected and frozen. Tissue sections were prepared and analyzed by radioimaging. For gastrointestinal tract and feces analyses, scintillation liquid counting was applied to determine the quantity of radioactivity. Organs of the gastrointestinal tract (esophagus, stomach, small and large intestine) were solubilized with a ratio of 100 mg of sample to 1 mL of tetramethylammonium hydroxide (TMAH, 25% in H_2O) for 3 h at 60 °C and for feces with a ratio of 100 mg of sample to 2 mL of TMAH. Once the solution became completely clear and homogeneous, 10 to 50 μL of sample was added to 5 mL of Ultima Gold Cocktail from PerkinElmer, and the radioactivity was counted in a liquid scintillation counter (TRI-CARB 2100TR, Packard).

Intravenous Injection. Mice (n = 4) were exposed by intravenous injection to 1 μg of ^{14}C- MWCNTs (14.8×10^3 Bq) suspended in dispersion medium (50 μL) and sacrificed 4 days after exposure. Organs were processed and analyzed as described for the pharyngeal aspiration study.

Quantification of MWCNTs in Organs. Radioimaging Counting. Fifty tissue sections were used for each organ to ensure sufficient sampling. These sections were analyzed by radioimaging to determine the Bq/per tissue section volume, which was converted to total radioactivity per organ on the basis of the total volume of each organ (determined by organ weighing).

Liquid Scintillation Counting. This method involved extracting MWCNTs from organs and radioactivity counting by liquid scintillation. The quantitative recovery of the procedure was first validated by spiking samples of each organ (lung, liver, and spleen) with a known amount of ^{14}C MWCNTs and evaluating recovery. The quantities of MWCNTs for these tests (1 to 20 ng per 100 mg of spleen and liver and 1 to 20 μg for lung) were selected according to estimates deduced from the radioimaging signals observed in corresponding tissue sections. Samples of 100 mg of organs containing MWCNTs were mixed with 1 mL of TMAH (25 wt % in H_2O) for 3 h at 60 °C. Once the solution became completely clear and homogeneous, 10 μL of sample was added to 5 mL of Ultima Gold Cocktail from PerkinElmer, and the radioactivity was counted in a liquid scintillation counter (TRI-CARB 2100TR, Packard). Extraction was quantitative for each sample, as shown by the slope of 1 when experimental recovered quantities of MWCNTs were plotted against theoretical values (S6, Supporting Information). These tests demonstrated that determination of MWCNT quantity was reliable for samples containing 5 to 100 ng of MWCNTs per 100 mg of organ. Below 5 ng, only radioimaging allowed satisfactory analysis of the amounts of MWCNTs in organs. For liver and spleen, radioimaging and liquid scintillation methods provided very similar results, with an uncertainty of ±10%. In contrast, for lung, radioactivity counting systematically gave lower values than the scintillation method for the amounts of radioactivity present; this was probably due to the nonhomogeneous distribution of the labeled MWCNTs.

Thin-Layer Chromatograms. TLC was performed on silica gel aluminum support (Sigma-Aldrich, 91835-50EA) using chloroform–ethyl acetate–acetic acid (80/20/1) as migration solvent.

Blood Analysis. Blood samples (whole blood cells included) were collected from the abdominal aortic vein from each animal. Aliquots of 1 μL were deposited on glass slides, and the radioactivity was quantitatively counted by radioimaging (detection threshold, 0.2 pg/μL).

Urine Analysis. One day before sacrifice, animals (4 animals/time point) were housed in metabolic cages for 24 h and urine was collected. Aliquots of 1 μL of urine were deposited on glass slides, and the radioactivity was counted by radioimaging.

Histopathology. Animals were healthy during this study, with normal weight evolution. Five histological sections of lungs, two sections of liver, and two sections of spleen from mice at day 30, 180, and 360 after lung exposure were mounted on glass slides and submitted to a pathologist. The sections were stained with hematoxylin and eosin. The quality of the histological sections was considered adequate for the purposes of the study. There were no treatment-related histological findings. The microscopic findings were those commonly seen in the laboratory mouse. There was no evidence of test item related inflammatory process.

HRTEM Analyses of MWCNTs Extracted from Organs. Organ extracts were prepared with TMAH as described above, and the MWCNTs were concentrated by centrifugation for 2 h at 55 000 rpm/186000g in an Optima MAX-XP Ultracentrifuge from Beckman Coulter. The pellets were suspended in TMAH at 70 °C and centrifuged again in similar conditions. The pellets were then washed twice with a denaturating solution of 8 M urea in 100 mM Tris pH 8.5 to remove traces of biological components and centrifuged again. The supernatant was discarded, and the solid phase was resuspended in a small volume of the denaturing solution and analyzed by TEM. Radioactivity counting by radioimaging was used to confirm the presence of MWCNTs at each step of the extraction protocol. Aliquots of resuspended MWCNTs were mounted on copper grids (Formvar 400 Mesh, ELOISE, France) and dried, and remaining traces of crystallized urea were sublimated at 180 °C (in an oil bath) under vacuum. The grids were checked by optical microscopy and radioactivity counting to verify the presence of MWCNTs. TEM images were obtained on a Jeol 2200FS microscope working at an accelerating voltage of 200 keV and equipped with an ultra-high resolution (UHR) pole-piece, allowing a resolution of 0.19 nm (point to point) in the HRTEM mode, and with a Gatan US1000 slow-scan CCD camera and an EDX system.

Conflict of Interest: The authors declare no competing financial interest.

Acknowledgment. This work was supported by the CEA program Toxicology, the European NANOGENOTOX Joint Action (Grant Agreement no. 2009 21), ANSES (project Bio14CNT), the European Union's Seventh Framework Programme for research, technological development and demonstration under grant agreement no. 310451, and Nanotoxicology Transversal Program of CEA. We thank Sami Habib, who was involved in the CVD setup for the ^{14}C-labeled MWCNT synthesis; C. Mallet, O. Rabouille, and B. Verhaeghe (CEA/DEN-SEMI/LLM2E) for SEM and TEM analyses on pristine ^{14}C-labeled MWCNT, Marie Carrière for contributing to developing the dispersion protocol (CEA-INAC, LSDRM), and the DSV-iBiTec-S TEM team.

Supporting Information Available: Figure S1: Comparative radioactivity levels in tissue sections of liver, spleen, bone morrow, and kidney from day 1 to day 360 postexposure. Figure S2: Thin-layer chromatography analysis of spleen and liver tissue extracts (180 and 360 days postexposure), as compared to ^{14}C-2,4-dimethoxybenzoic acid. Figure S3: Radioimaging of heart, brain, and thymus tissue sections at day 360 postexposure. Figure S4: Comparison between gavage and lung MWCNT exposure. Figure S5: Spleen, liver, and lung distribution after intravenous injection of MWCNTs at day 1 postadministration. Figure S6: Recovery of MWCNTs after spiking MWCBTS in liver, spleen, and lung tissue extracts. This material is available free of charge *via* the Internet at http://pubs.acs.org.

Note Added after ASAP Publication: This paper was published ASAP on May 28, 2014. The Acknowledgment section was corrected and the revised version was reposted on June 6, 2014.

REFERENCES AND NOTES

1. Ajayan, P. M.; Tour, J. M. Materials Science: Nanotube Composites. *Nature* **2007**, *447*, 1066–1068.
2. Kostarelos, K.; Bianco, A.; Prato, M. Promises, Facts and Challenges for Carbon Nanotubes in Imaging and Therapeutics. *Nat. Nanotechnol.* **2009**, *4*, 627–633.
3. Helland, A.; Wick, P.; Koehler, A.; Schmid, K.; Som, C. Reviewing the Environmental and Human Health Knowledge Base of Carbon Nanotubes. *Environ. Health Perspect.* **2007**, *115*, 1125–1131.
4. Castranova, V.; Schulte, P. A.; Zumwalde, R. D. Occupational Nanosafety Considerations for Carbon Nanotubes and Carbon Nanofibers. *Acc. Chem. Res.* **2013**, *46*, 642–649.
5. Donaldson, K.; Aitken, R.; Tran, L.; Stone, V.; Duffin, R.; Forrest, G.; Alexander, A. Carbon Nanotubes: A Review of their Properties in Relation to Pulmonary Toxicology and Workplace Safety. *Toxicol. Sci.* **2006**, *92*, 5–22.

6. Kayat, J.; Gajbhiye, V.; Tekade, R. K.; Jain, N. K. Pulmonary Toxicity of Carbon Nanotubes: A Systematic Report. *Nanomedicine* **2011**, *7*, 40–49.
7. Shvedova, A. A.; Kisin, E. R.; Porter, D.; Schulte, P.; Kagan, V. E.; Fadeel, B.; Castranova, V. Mechanisms of Pulmonary Toxicity and Medical Applications of Carbon Nanotubes: Two Faces of Janus? *Pharmacol. Ther.* **2009**, *121*, 192–204.
8. Porter, D. W.; Hubbs, A. F.; Mercer, R. R.; Wu, N.; Wolfarth, M. G.; Sriram, K.; Leonard, S.; Battelli, L.; Schwegler-Berry, D.; Friend, S.; *et al*. Mouse Pulmonary Dose- and Time Course-Responses Induced by Exposure to Multi-Walled Carbon Nanotubes. *Toxicology* **2010**, *269*, 136–147.
9. Rothen-Rutishauser, B.; Brown, D. M.; Piallier-Boyles, M.; Kinloch, I. A.; Windle, A. H.; Gehr, P.; Stone, V. Relating the Physicochemical Characteristics and Dispersion of Multi-walled Carbon Nanotubes in Different Suspension Media to their Oxidative Reactivity in Vitro and Inflammation in Vivo. *Nanotoxicology* **2010**, *4*, 331–342.
10. Li, Z.; Hulderman, T.; Salmen, R.; Chapman, R.; Leonard, S. S.; Young, S. H.; Shvedova, A.; Luster, M. I.; Simeonova, P. P. Cardiovascular Effects of Pulmonary Exposure to Single-Wall Carbon Nanotubes. *Environ. Health Perspect.* **2007**, *115*, 377–382.
11. Liu, Y.; Zhao, Y.; Sun, B.; Chen, C. Understanding the Toxicity of Carbon Nanotubes. *Acc. Chem. Res.* **2013**, *46*, 702–713.
12. Zhou, H.; Mu, Q.; Gao, N.; Liu, A.; Xing, Y.; Gao, S.; Zhang, Q.; Qu, G.; Chen, Y.; Liu, G.; *et al*. A Nano-Combinatorial Library Strategy for the Discovery of Nanotubes with Reduced Protein-Binding, Cytotoxicity, and Immune Response. *Nano Lett.* **2008**, *8*, 859–865.
13. Gasser, M.; Rothen-Rutishauser, B.; Krug, H. F.; Gehr, P.; Nelle, M.; Yan, B.; Wick, P. The Adsorption of Biomolecules to Multi-Walled Carbon Nanotubes is Influenced by both Pulmonary Surfactant Lipids and Surface Chemistry. *J. Nanobiotechnol.* **2010**, *8*, 31.
14. Kreyling, W. G.; Semmler-Behnke, M.; Seitz, J.; Scymczak, W.; Wenk, A.; Mayer, P.; Takenaka, S.; Oberdorster, G. Size Dependence of the Translocation of Inhaled Iridium and Carbon Nanoparticle Aggregates from the Lung of Rats to the Blood and Secondary Target Organs. *Inhalation Toxicol.* **2009**, *21* (Suppl 1), 55–60.
15. Aiso, S.; Kubota, H.; Umeda, Y.; Kasai, T.; Takaya, M.; Yamazaki, K.; Nagano, K.; Sakai, T.; Koda, S.; Fukushima, S. Translocation of Intratracheally Instilled Multiwall Carbon Nanotubes to Lung-Associated Lymph Nodes in Rats. *Ind. Health* **2011**, *49*, 215–220.
16. Porter, D. W.; Hubbs, A. F.; Chen, B. T.; McKinney, W.; Mercer, R. R.; Wolfarth, M. G.; Battelli, L.; Wu, N.; Sriram, K.; Leonard, S.; *et al*. Acute Pulmonary Dose-Responses to Inhaled Multi-Walled Carbon Nanotubes. *Nanotoxicology* **2013**, *7*, 1179–1194.
17. Ryman-Rasmussen, J. P.; Cesta, M. F.; Brody, A. R.; Shipley-Phillips, J. K.; Everitt, J. I.; Tewksbury, E. W.; Moss, O. R.; Wong, B. A.; Dodd, D. E.; Andersen, M. E.; *et al*. Inhaled Carbon Nanotubes Reach the Subpleural Tissue in Mice. *Nat. Nanotechnol.* **2009**, *4*, 747–751.
18. Mercer, R. R.; Hubbs, A. F.; Scabilloni, J. F.; Wang, L.; Battelli, L. A.; Schwegler-Berry, D.; Castranova, V.; Porter, D. W. Distribution and Persistence of Pleural Penetrations by Multi-Walled Carbon Nanotubes. *Part. Fibre Toxicol.* **2010**, *7*, 28.
19. Stapleton, P. A.; Minarchick, V. C.; Cumpston, A. M.; McKinney, W.; Chen, B. T.; Sager, T. M.; Frazer, D. G.; Mercer, R. R.; Scabilloni, J.; Andrew, M. E.; *et al*. Impairment of Coronary Arteriolar Endothelium-Dependent Dilation after Multi-Walled Carbon Nanotube Inhalation: a Time-Course Study. *Int. J. Mol. Sci.* **2012**, *13*, 13781–13803.
20. Mercer, R. R.; Scabilloni, J. F.; Hubbs, A. F.; Wang, L.; Battelli, L. A.; McKinney, W.; Castranova, V.; Porter, D. W. Extrapulmonary Transport of MWCNT Following Inhalation Exposure. *Part. Fibre Toxicol.* **2013**, *10*, 38.
21. Deng, X.; Wu, F.; Liu, Z.; Luo, M.; Li, L.; Ni, Q.; Jiao, Z.; Wu, M.; Liu, Y. The Splenic Toxicity of Water Soluble Multi-Walled Carbon Nanotubes in Mice. *Carbon* **2009**, *47*, 1421–1428.
22. Petersen, E. J.; Huang, Q.; Weber, W. J. Ecological Uptake and Depuration of Carbon Nanotubes by Lumbriculus Variegatus. *Environ. Health Perspect.* **2008**, *116*, 496–500.
23. Pinault, M.; Mayne-L'hermite, M.; Reynaud, C.; Pichot, V.; Launois, P.; Ballutaud, D. Growth of Multi-Walled Carbon Nanotubes During the Initial Stages of Aerosol-Assisted CCVD. *Carbon* **2005**, *43*, 2968–2976.
24. Castro, C.; Pinault, M.; Porterat, D.; Reynaud, C.; Mayne-L'hermite, M. The Role of Hydrogen in the Aerosol-Assisted Chemical Vapor Deposition Precess in Producing Thin and Densily Packed Vertically Aligned Carbon Nanotubes. *Carbon* **2013**, *61*, 585–594.
25. Porter, D. W.; Sriram, K.; Wolfarth, M. G.; Jefferson, A.; Schwegler-Berry, D.; Andrew, M. E.; Castranova, V. A Biocompatible Medium for Nanoparticle Dispersion. *Nanotoxicology* **2008**, *2*, 144–154.
26. Driscoll, K. E.; Costa, D. L.; Hatch, G.; Henderson, R.; Oberdorster, G.; Salem, H.; Schlesinger, R. B. Intratracheal Instillation as an Exposure Technique for the Evaluation of Respiratory Tract Toxicity: Uses and Limitations. *Toxicol. Sci.* **2000**, *55*, 24–35.
27. Dive, V.; Andarawewa, K. L.; Boulay, A.; Matziari, M.; Beau, F.; Guerin, E.; Rousseau, B.; Yiotakis, A.; Rio, M. C. Dosing and Scheduling Influence the Antitumor Efficacy of a Phosphinic Peptide Inhibitor of Matrix Metalloproteinases. *Int. J. Cancer* **2005**, *113*, 775–781.
28. Allen, B. L.; Kotchey, G. P.; Chen, Y.; Yanamala, N. V.; Klein-Seetharaman, J.; Kagan, V. E.; Star, A. Mechanistic Investigations of Horseradish Peroxidase-Catalyzed Degradation of Single-Walled Carbon Nanotubes. *J. Am. Chem. Soc.* **2009**, *131*, 17194–17205.
29. Kagan, V. E.; Konduru, N. V.; Feng, W.; Allen, B. L.; Conroy, J.; Volkov, Y.; Vlasova, I. I.; Belikova, N. A.; Yanamala, N.; Kapralov, A.; *et al*. Carbon Nanotubes Degraded by Neutrophil Myeloperoxidase Induce Less Pulmonary Inflammation. *Nat. Nanotechnol.* **2010**, *5*, 354–359.
30. Taylor, A. E.; Gaar, K. A., Jr. Estimation of Equivalent Pore Radii of Pulmonary Capillary and Alveolar Membranes. *Am. J. Physiol.* **1970**, *218*, 1133–1140.
31. Conhaim, R. L.; Eaton, A.; Staub, N. C.; Heath, T. D. Equivalent Pore Estimate for the Alveolar-Airway Barrier in Isolated Dog Lung. *J. Appl. Physiol.* **1988**, *64*, 1134–1142.
32. Kreyling, W. G.; Hirn, S.; Moller, W.; Schleh, C.; Wenk, A.; Celik, G.; Lipka, J.; Schaffler, M.; Haberl, N.; Johnston, B. D.; *et al*. Air-Blood Barrier Translocation of Tracheally Instilled Gold Nanoparticles Inversely Depends on Particle Size. *ACS Nano* **2014**, *8*, 222–233.
33. Mitchell, L. A.; Lauer, F. T.; Burchiel, S. W.; McDonald, J. D. Mechanisms for How Inhaled Multiwalled Carbon Nanotubes Suppress Systemic Immune Function in Mice. *Nat. Nanotechnol.* **2009**, *4*, 451–456.
34. Novoselov, K. S.; Fal'ko, V. I.; Colombo, L.; Gellert, P. R.; Schwab, M. G.; Kim, K. A Roadmap for Graphene. *Nature* **2012**, *490*, 192–200.
35. Georgin, D.; Czarny, B.; Botquin, M.; Mayne-L'hermite, M.; Pinault, M.; Bouchet-Fabre, B.; Carriere, M.; Poncy, J. L.; Chau, Q.; Maximilien, R.; *et al*. Preparation of (14)C-Labeled Multiwalled Carbon Nanotubes for Biodistribution Investigations. *J. Am. Chem. Soc.* **2009**, *131*, 14658–14659.